WILEY | Hindawi

Research Article

Formulating Polypropylene with Desired Mechanical Properties through Melt Compounding of Homopolymer and Impact Copolymer

Yucheng Peng [iD],[1] Shaoyang Liu [iD],[2] Pixiang Wang,[2] Yifen Wang,[3] and Xueqi Wang[1]

[1]*College of Forestry and Wildlife Sciences, Auburn University, Auburn, AL 36849, USA*
[2]*Center for Materials and Manufacturing Sciences, Departments of Chemistry and Physics, Troy University, Troy, AL 36082, USA*
[3]*Department of Biosystems Engineering, Auburn University, Auburn, AL 36849, USA*

Correspondence should be addressed to Yucheng Peng; yzp0027@auburn.edu and Shaoyang Liu; lius@troy.edu

Many grades of homopolymer polypropylene (HPP) and impact copolymer PP (ICPP) with a wide range of mechanical properties have been developed for a variety of applications in different industrial sectors. Management of this wide range of materials is a challenge for material suppliers and manufacturers and product developers. This research was to provide insights for managing material supplies through formulating PP with specific mechanical properties using melt compounding of ICPP and HPP. ICPP and HPP were compounded with an internal mixer at different ratios and then the mixtures were injection molded into specimens for characterization. The mechanical behaviors, fracture surfaces, and thermal properties of the mixtures were then characterized. The fracture surface results indicated that the morphologies of the rubber particles in ICPP changed after compounding with HPP, leading to different mechanical and thermal behaviors of the mixtures. Notched and unnotched impact strengths increased linearly with increasing ICPP contents. The crystallization peak temperatures increased linearly with increasing ICPP contents while the degrees of crystallinity of the mixtures decreased linearly. The thermal compounding process and the original material properties mainly determine the final mixture behaviors, and the mixture properties can be predicted based on the weight ratios of the two components.

1. Introduction

Polypropylene (PP) possessing desired mechanical properties, especially a required impact strength at a specific temperature, is critical for many applications in different industrial sectors, including packaging, construction, and automotive. The importance of different requirements on the mechanical properties of PP can be demonstrated by a variety of commercial grades of PP offered by many suppliers on the market. The applications of commercial homopolymer PP (HPP) are limited by its relatively low impact strength and high brittleness temperature. The brittleness of HPP can be modified using different strategies [1–8]. Blending HPP with a variety of particles, including rigid and rubber forms, has been demonstrated as an effective, simple, and economic way to optimize the material properties such

as impact strength. The most common way in the industry is to include elastomers/rubbers in homopolymer PP to enhance the impact strength, generating various grades of impact copolymer PP (ICPP) which have been commercialized successfully and dominate a large portion of the PP market [4–6]. The most used categories of elastomers/rubbers include ethylene-propylene rubbers (EPR) [9], butyl rubber [10], styrene-butadiene-styrene (SBS) copolymer [11, 12], and ethylene-propylene-diene (EPDM) copolymer [13].

The effect on impact properties of HPP differs with different elastomer/rubbers. The most effective impact strength enhancement can be achieved through embedding EPR or EPDM particles in the HPP matrix [6, 9, 14, 15] in a specific loading level range determined by final applications. Moderate impact strength improvement of HPP can also be

obtained when SBS and butyl rubber are used [15, 16]. The principles of increasing the impact strength of HPP by including elastomer/rubbers have been studied for many years and several mechanisms were proposed. The major theories attribute toughening mechanisms to the multiple-crazing, shear yielding, and rubber cavitation, depending on the properties of the matrix in which rubber particles are dispersed [2, 4, 6]. However, different theories have been applied to interpret the increased toughness in different cases with a variety of polymer matrices and rubber particles involved. No single toughening theory can explain all the phenomena observed for the enhancement in impact strength of HPP with the addition of rubber particles. Matrix shear yielding and rubber cavitation were reported to be a combined effect on toughening HPP when rubber particles are included in HPP. The dominant factor affecting the toughness of HPP is determined by the plastic deformation of the matrix polymer and rubber particles. When a brittle failure mode occurs for the polymer matrix, the formation of micro void and cavitation mechanism determines the toughness of the matrix material. Matrix shear yielding occurs first when the polymer matrix fails in a ductile mode. At different strain rates, the plastic deformation mechanisms of polymer matrix during failure are also different. Crazing is favored at high strain rates for rubber-modified HPP and matrix shear yielding is more popular at a lower strain rate. Under such circumstances, the failure behaviors of the material under tensile load with a low strain rate differ from those under a higher strain rate of impact testing condition. In addition to promoting crazing and shear yielding, including rubber particles can also change the cooling behaviors of polymer matrix after production, changing the fracture behavior of the binary system by changing the crystalline structures [6].

The effects of rubber particle characteristics, including shape, size, size distribution, and loading level, on the impact strength of HPP are also significant [2, 4, 6, 17, 18]. When the rubber particle loading level is too low, external stress is mainly applied to the matrix polymer. The toughening effect of rubber particles is limited. On the other hand, the toughening effect decreases when the rubber particle loading level increases to some extent. This is caused by the interactions among the rubber particles when they are approaching each other closely. In addition, the toughening mechanisms, including crazing, shear yielding, and rubber cavitation, have a limited effect on less amount of polymer matrix in the binary system, lowering the toughening functionality of the rubber particles. The effect of rubber particle size on toughening PP matrix was studied, and the optimal rubber particle size for toughening PP appears to be in a range of 0.1–0.5 μm[6].

Research results also indicate that small rubber particles can enhance the toughness of the matrix to a higher level than that of larger particles [2]. However, small rubber particles are not always better than large particles regarding the toughening effect. A relatively large size of rubber particle could block the propagation of the fracture front, changing the fracture path around the particle. The fracture path change can improve the toughness of the system. When the rubber particle size is smaller than the fracture ligament at the end of a fracture front, the existence of the particle around the front of the fracture only changes the rheological properties of the matrix and cannot influence the propagation of the fracture [4, 6, 18, 19]. The toughness of the system will not be impacted.

An effective method dispersing rubber particles evenly in HPP can be achieved through an in-reactor blending technology which involves polymerizing propylene first and then copolymerizing propylene with ethylene to form the rubber part of the product in situ [5, 20–22]. The mechanism of the in-reactor blending technology is complex and exhibits good impact-resistant properties due to the unique microstructures of the multiphase copolymer system. For different applications, a variety of in-reactor blends with different toughness are necessary to be prepared. The enlarged materials portfolio requirements on the converting side complicate the supply chain system for upstream materials producers and downstream converters and customers, increasing materials management costs for all the parties. From the perspective of materials suppliers and converters, there is a need to simplify the materials portfolio and better manage the material inventory in-house.

The objective of this study was to understand whether an in-house mechanical blending technology applied on a mixture of a grade of HPP and a grade of in-reactor ICPP could formulate PP with specific mechanical properties, focusing on the toughness of the mixture. A high rubber particle content in-reactor ICPP was mixed with a grade of HPP in different ratios, including weight ratios of ICPP to HPP at 100 : 0, 80 : 20, 60 : 40, 40 : 60, 20 : 80, and 0 : 100. The goal was to minimize material inventory for all the stakeholders through an in-house mechanical blending using an extrusion process. The effect of different rubber contents achieved by diluting ICPP using HPP on the mechanical properties of the mixture system was investigated. Additionally, mixing ICPP with HPP also offers insights for recycling different streams of PP regarding the mechanical behaviors of the recycled materials. During the dilution process, the rubber particle morphologies change and their impact on the mechanical and thermal properties of the mixtures was evaluated.

2. Experimental

2.1. Materials and Sample Preparation. Two grades of PP, ICPP (ExxonMobil™ PP7684KNE1) and HPP (ExxonMobil™ PP1264E1), were provided by ExxonMobil Chemical Company (Houston, TX) for this research. Both HPP and ICPP have a density of 0.9 g/cm^3. Based on the material property datasheet, the melt mass-flow rate (MFR) of HPP and ICPP is 20 and 19 g/10 minutes when measured using the conditions of 230°C/2.16 kg.

The mixing of ICPP and HPP followed a procedure described in a previous publication [23]. Melt compounding of ICPP and HPP was conducted using a C.W. Brabender internal mixer (CWB-2128, Hackensack, NJ) at 200°C. Before compounding, HPP and ICPP pellets were dry blended based on the designed weight ratios. The weight ratios used

in this study were 0, 20, 40, 60, 80, and 100 wt.% of ICPP in the total mixture weight. During the compounding process, mixtures of HPP and ICPP pellets were melted first with the two rollerblades of the mixer counterrotating at 60 rpm, followed by mixing in the barrel under the shear force generated by the two roller blades for five more minutes. After the melt compounding, the mixture melt was scraped off the mixer when they were still in melt status and then was let in room conditions to be solidified.

After solidification, the mixtures were ground into pellets using a low-speed granulator (Shini Plastic Technologies Inc., Willoughby, OH) loaded with a three-millimeter-opening sieve. The mixture pellets were then injection molded into testing specimens according to the ASTM standards D638 (type I), D790, and D256 using a benchtop injection molding machine (Medium Machinery, LLC., Woodbridge, VA). The injection molding production of all the specimens was performed at a temperature of 200°C and a pressure of 90 MPa. After injection, a packing pressure of 90 MPa was applied for five seconds to cool the melt in the aluminum molds. The pure ICPP and HPP pellets went through the same mixing procedures and were used as the control samples, which were designated as the samples with ICPP contents of 100% and 0% by weight.

2.2. Characterization

2.2.1. Mechanical Properties.
Mechanical properties of the injection-molded specimens, including tensile, flexural, and impact properties, were measured according to ASTM standards of D638, D790, and D256. All the mechanical tests were performed in a room at a temperature of 23 ± 2°C and relative humidity (RH) of 50 ± 5%.

Tensile properties of all the specimens were characterized using a Mark-10 ESM750s (Copiague, NY) motorized test stand and a 2500-N load cell with a load resolution of ±0.15% was used to record the tensile force. An axial extensometer Model 3542 from Epsilon Technology Corporation (Jackson, WY) was used to measure the tensile strain during the test. A testing speed of five mm/min and a strain rate at the start of the test of 0.1 minute^{-1} were employed. The tensile strength, modulus of elasticity (MOE), and percentage of elongation (strain) at yield were reported for all the specimens.

The measurement of the flexural properties of all the mixtures was conducted using the mark-10 motorized test stand attached with a 500-N load cell. Both procedures A and B specified in ASTM D790 were used to test the specimens. The outer fiber strain rates for procedures A and B are 0.01 and 0.1 minute^{-1}, respectively. All the specimens that did not yield or break with the outer fiber strain rate of 0.1 minute^{-1} (the test procedure B) and the flexural properties (flexural strength and MOE) were collected at 5% strain using the test procedure B.

Izod impact testing specimens were notched according to ASTM D256 using a manual CEAST notcher from Instron (Norwood, MA), and the impact tests were conducted on an XJUD Digital Charpy Izod Impact testing machine (Deli Group Co. Ltd., Ningbo, China). The impact strengths were obtained for both notched and unnotched Izod impact tests. The energy breaking the impact specimens was recorded with a resolution of 0.01 J.

Five replicates were measured for tensile and flexural properties, and ten replicates were used to obtain the Izod impact strengths for each sample. Statistical analysis through a one-way analysis of variance (ANOVA) of the mechanical properties was performed using SAS to compare among different samples and a significance level of 0.05 was used.

2.2.2. Melt Flow Rate.
The MFR values of all the mixtures were measured using a melt flow rate tester (Techtongda, Markham, ON, Canada) according to the ASTM D1238 using the pellet samples obtained from the granulator. The measurements were conducted at 230°C with a deadweight of 2.16 kg. The extrudate cut-off time-interval was wet for up to 30 seconds for all the specimens. Five replicates were collected for each sample and weighed to the nearest 1 mg. The standard MFR with the units of g/10 min was reported. The same statistical analysis procedure was also applied to analyze the melt flow rate.

2.2.3. Scanning Electron Microscopy (SEM).
The fracture surfaces of impact tested specimens for all the mixtures were characterized by SEM. Before the SEM examination, the fracture surface was sputter-coated with gold for 60 seconds in a Q150R ES sputter coating device from Electron Microscopy Sciences (Hatfield, PA, US). The SEM characterization of the fracture surface was performed using a Zeiss Evo 50VP scanning electron microscope (Oberkochen, Germany) at an accelerating voltage of 20 kV.

2.2.4. Thermal Properties.
Thermal properties characterization of all the mixtures was conducted through differential scanning calorimetry (DSC) and thermogravimetric analysis (TGA). The DSC measurements were carried out using a differential scanning calorimeter of DSC-250 (TA Instruments, DE, USA). A mixture of around 10–15 mg was used in each DSC measurement. Five steps were included in the DSC measurement: (1) heating the sample from 40°C to 200°C at a heating rate of 10°C/min, (2) isothermal for two minutes at 200°C, (3) cooling the sample from 200°C to 40°C at a cooling rate of 5°C/min, (4) isothermal for two minutes at 40°C, and (5) heating the sample from 40°C to 200°C at the heating rate of 10°C/min. Each sample was measured in triplicate. The data analysis was performed with the TRIOS software (TA Instruments, DE, UDA) to obtain the parameters of melting and crystallization of the mixtures.

The TGA was conducted under nitrogen using a thermogravimetric analyzer of TGA-550 (TA Instruments, DE, USA). A nitrogen flow rate of 60 ml/min was used for sample purge and 40 ml/min for balance purge. A sample with a weight between 10 and 15 mg was used for all the measurements. All the specimens were heated from 40°C to 600°C using a temperature ramp rate of 5°C/min. Each sample was tested three times, and the software of TRIOS

(TA Instruments, DE, USA) was used to analyze the TGA curves.

3. Results and Discussion

3.1. Tensile and Flexural Properties. The tensile properties of the HPP and ICPP mixtures with different ICPP weight percentages of 0, 20, 40, 60, 80, and 100 wt.% are shown in Figure 1. The detailed numbers and the statistical analysis results are shown in Table 1. Different letters of A, B, C, D, and E in Table 1 demonstrate significant differences in the mechanical properties, including tensile MOE, strength, and strain at yield. After processing with the batch mixer, the tensile MOE and strength of HPP are 1.58 GPa and 32.47 MPa, while the corresponding numbers for ICPP are 1.34 GPa and 19.88 MPa, respectively (Figure 1 and Table 1). The tensile MOE and strength of ICPP are significantly lower than those of HPP (Table 1). According to the rule of mixtures, adding ICPP in HPP would decrease the tensile MOE and strength. As shown in Figure 1 and Table 1, adding 20, 40, 60, and 80 wt.% ICPP into HPP decreased the tensile MOE to 1.50, 1.52, 1.45, 1.45 GPa. Simultaneously, the tensile strengths of the mixtures with 20, 40, 60, and 80 wt.% ICPP, which are 29.94, 28.53, 25.15, and 24.66 MPa, are also significantly lower than those of HPP (32.47 MPa). The tensile strain at yield decreased from 9.95% to 8.62, 7.51, 5.87, 5.60, and 4.77% as the ICPP content in the mixtures increased from 0 wt.% to 20, 40, 60, and 100%.

ICPP consists of two different phases of materials: PP homopolymer phase and rubber particles. Rubber particles are evenly dispersed and distributed in the PP homopolymer phase in ICPP which is achieved by an in-reactor blending technology [24–26]. The PP homopolymer phase in ICPP may have different properties than those of HPP used in this study, such as molecular weight and its distribution. When mixing HPP with ICPP, the homopolymer phase in ICPP would be miscible with the HPP, and changes in the mechanical behaviors of the final mixtures would be expected. That is the first factor to be considered for the mechanical properties of the mixtures.

The second effect would be associated with the behavior changes of the rubber particles originally dispersed in ICPP, such as the rubber particle concentration, morphology, size distribution, and dispersion and distribution in the newly formed mixture matrix.

The tensile testing specimens were obtained by cooling down the injection molded parts naturally to room temperature from 200°C. During the cooling process, the mixtures crystallized, and shrinkage of the specimens was observed. Simultaneously, mismatching thermal expansion coefficients of the PP homopolymer phase and rubber particles resulted in thermal stresses near the rubber-polymer interface [27]. Under this circumstance, residual compression stresses and strains applied to the rubber particles by the PP homopolymer phase were frozen into the specimen. A schematic representation of the stresses around rubber particles is shown in Figure 2(a). When a tensile load is applied to the specimen, internal tensile stresses are generated in the load direction which offset the compression

stresses applied to the rubber particles in the same direction. Simultaneously, a compression stress is also generated in the cross direction of the specimen, resulting in a larger compression stress to the rubber particles across the tensile load direction. As the tensile load increases, initial elastic deformation along the load direction occurs to the homopolymer matrix and the dispersed rubber particles. In this phase of elastic deformation, no phase separation occurred between the rubber particles and homopolymer matrix (Figure 2(b)). According to the rule of mixtures, the moduli of the mixtures would be small than those of HPP and larger than those of ICPP (Figure 1 and Table 1). The interference of rubber particles on the elastic behavior of the mixtures also depends on the loading levels of the rubber particles. Adding 20 and 40 wt.% ICPP into HPP decreased the MOE by around 5% and the addition of 60 and 80 wt.% ICPP reduced the MOE to a level which is around 8% lower than that of HPP (Table 1).

As the tensile load continues to increase to a critical point that the internal stress is greater than the interfacial bonding strength between the rubber particles and homopolymer matrix, at this moment, a phase separation between rubber particles and homopolymer matrix occurs near the interface at the farthest end of the rubber particle (Figure 2(c)). At this point, plastic deformation starts in the mixture. The assumption for this to occur is that the interfacial bonding strength is smaller than that of the cohesive strength of the homopolymer matrix. If this is not the case, there will be no phase separation between rubber particles and the homopolymer matrix before the yielding of the homopolymer phase which is not true for this study. After the partial phase separation between the rubber particles and the matrix, the compression stress (the green arrows shown in Figure 2(c)) acting on the rubber particles continues to increase in a proportion to the applied external tensile load and this compression stress generates tensile stresses to the rubber particles along the tensile load direction (the white arrows shown in Figure 2(c)). The state of stresses of the rubber particles maintains until a point is reached where the yielding of the homopolymer phase is achieved (the red arrows in Figure 2(d)). The tensile yield strength of the mixture is obtained at this point.

During the tensile testing process, MOE is a characteristic of the mixture in the elastic deformation zone which is impacted by the rubber particles and the homopolymer matrix. Adding rubber particles lowered the MOE of the mixture (Table 1) due to the lower stiffness of the rubber particles. Depending on the rubber particle content, distribution, and particles size, the effect of the rubber particles on the MOE of the mixture varies. Adding 20 and 40 wt.% ICPP in HPP lowered the MOE for the mixture to a similar level (Table 1) which possibly indicates that the rubber particle morphologies dispersed in HPP at these two loading levels are similar. For the same reason, the morphologies of rubber particles when adding 60 and 80 wt.% of ICPP in HPP could be similar because the addition of 60 and 80 wt.% ICPP reduced the MOE to a similar level (Table 1). The SEM images characterizing the fracture surface of the mixture shown in Figure 3 verified the proposed theory. The observation from the SEM images
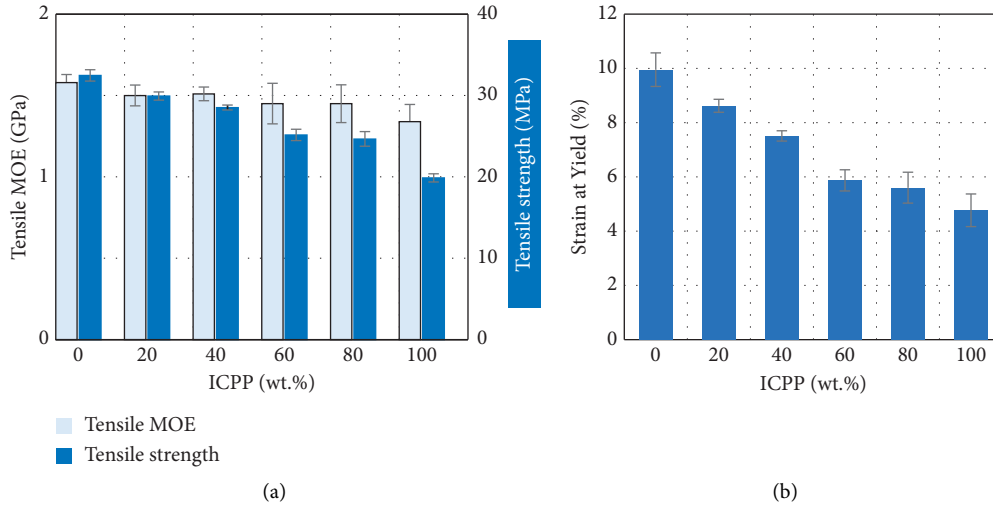
FIGURE 1: The tensile properties of the mixtures with different weight percentages of ICPP: (a) tensile MOE and strength and (b) strain at yield.

demonstrates that the rubber particles in the mixtures with 60 and 80 wt. % ICPP (Figures 3(d) and 3(e)) are much smaller than those with 20 and 40 wt. % ICPP (Figures 3(b) and 3(c)). Particle size analysis was performed on these SEM images, 55 particles were selected for each image, and the largest dimension of the particle was measured using ImageJ software (National Institutes of Health).

The rubber particles' sizes in the mixtures with 100, 80, 60, 40, and 20 wt.% ICPP are 2.04 ± 0.67, 1.08 ± 0.25, 1.69 ± 0.63, 2.52 ± 1.12, and $2.81 \pm 1.54\,\mu$m, respectively. Simultaneously, the fracture surface morphologies of pure HPP and ICPP are also shown in Figure 3. During the mixing process, rubber particles changed their morphologies under shearing forces, leading to different particle sizes after cooling. Different particles' sizes then impacted the elastic deformation in different ways, resulting in the different moduli of the mixtures as shown in Figure 1(a) and Table 1. At 60 and 80 wt.% ICPP loading, the rubber particles embedded in the mixture are much smaller in size than those in the mixture with 20 and 40 wt.% ICPP. At 20 and 40 wt.% ICPP, the rubber particles are similar in size when compared with rubber particles in pure ICPP (Figure 3).

A linear regression analysis of the tensile strength (Y) data showed that it decreased linearly with the weight percentage of ICPP (X) and the equation is shown as follows.

$$Z = -2.35X + 35.0,$$
$$R^2 = 0.96. \tag{1}$$

Based on the proposed mechanism shown in Figure 2(d), the tensile strength is mainly caused by the yielding of the homopolymer phase in the mixture. For the same size specimens, adding ICPP in the HPP replaced homopolymer phase in the mixture with rubber particles and the volumes of the replaced homopolymer were in proportion to the weight percentage of ICPP. Therefore, the volume of homopolymer yielded during the tensile testing decreased proportionally with the added weight of ICPP, resulting in the linear decrease of the tensile strength

shown in the experimental measurements. The same effect applies to the strain at yield Z for the mixtures and the data analysis demonstrates a similar linear relationship between the strain at yield and the ICPP weight percentage (X) as shown in

$$Z = -1.05X + 10.7,$$
$$R^2 = 0.97. \tag{2}$$

The flexural results using test procedure B according to ASTM D790 are shown in Figure 4 and Table 1. The statistical analysis of the data showed that the flexural MOE and strength of ICPP are significantly lower than those of HPP (Table 1). Adding ICPP into HPP significantly lowered the flexural MOE and strength. Adding 20 wt.% ICPP lowered the mixture flexural MOE and strength to the same level as adding 40 wt.% ICPP and adding 60 wt.% ICPP showed similar flexural properties as that of the mixture with 80 wt.% ICPP. The morphologies of the rubber particles in the mixture after mixing shown in Figure 3 are probably the reason causing the different flexural behaviors of the mixture with different contents of ICPP.

3.2. Impact Properties. The impact properties of the mixtures with different ICPP contents, including notched and unnotched impact strengths, are shown in Figure 5 and Table 1. One thing we need to clarify is that our impact strength values are significantly lower than the specifications in the datasheet from the supplier. The reasons could be associated with the specimens manufacturing and testing equipment. Our objective is to obtain the effect on material properties through mixing HPP and ICPP and tested results demonstrated that the goal has been achieved. The notched ($4.82\,kJ/m^2$) and unnotched ($102\,kJ/m^2$) impact strengths of ICPP are much higher than those of HPP, which are 1.62 and $55.4\,kJ/m^2$, respectively. For notched impact strength, adding 20 wt.% ICPP did not significantly change the property (Table 1). At 40, 60, and 80 wt.% of ICPP, the

TABLE 1: The mechanical properties of HPP, ICPP, and the ICPP and HPP mixtures.

Copolymer (wt.%)	Tensile properties						Flexural properties				Impact strength (kJ/m2)				Melt flow index (g/10 min)	
	MOE (MPa)		strength (GPa)		Strain (%)		MOE (GPa)		Strength (MPa)		Notched		Unnotched			
0	1.58	A[a]	32.5	A	9.95	A	1.68	A	52.5	A	1.62	E	55.4	B	15.9 ± 0.03[b]	D
20	1.50	B	29.9	B	8.62	B	1.58	B	49.9	B	1.67	E	62.0	B	16.5 ± 0.06	C/D
40	1.52	B	28.5	C	7.51	C	1.59	B	48.9	B	2.57	D	72.2	B	17.0 ± 0.04	C
60	1.45	C	25.2	D	5.87	D	1.48	C	44.4	C	3.76	C	92.5	A	19.4 ± 0.03	B
80	1.45	C	24.7	D	5.60	D	1.55	C	43.3	C	4.22	B	102	A	20.8 ± 0.04	A
100	1.34	D	19.9	E	4.77	E	1.35	D	38.2	D	4.82	A	102	A	19.9 ± 0.02	B

[a]The letters A, B, C, D, and E represent the significant levels in statistical analysis. The values with different letters are significantly different. [b]Standard deviation.
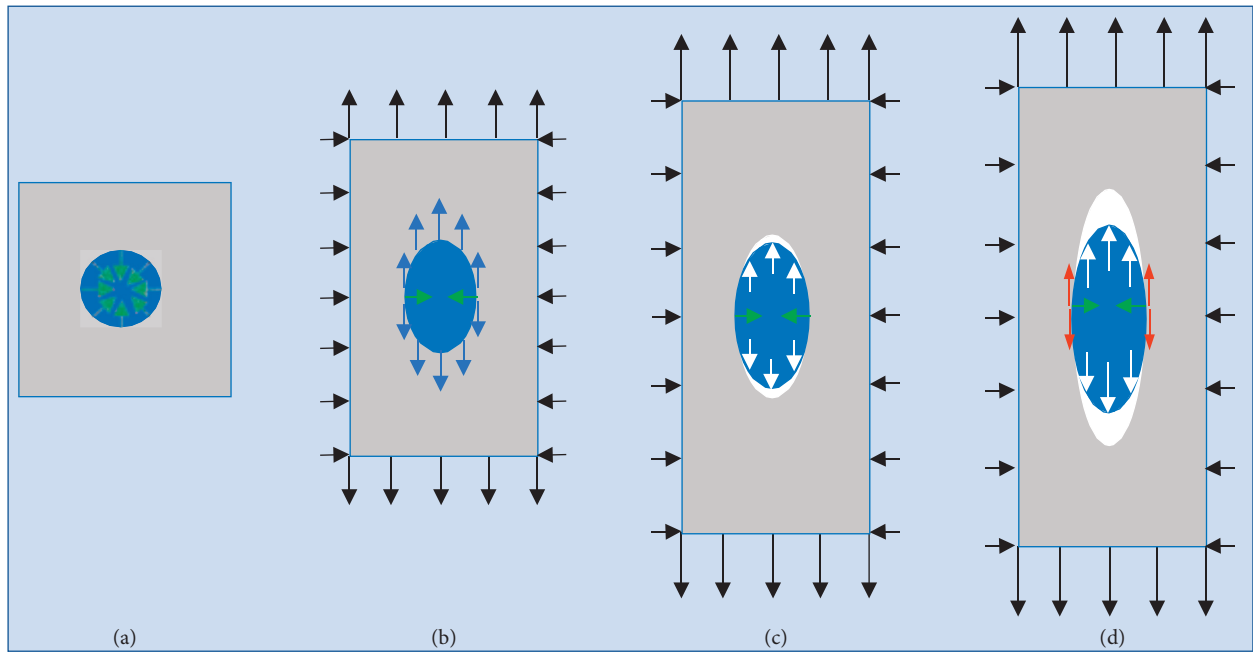
FIGURE 2: A schematic diagram of the tensile deformation of the mixture showing (a) the residual stress, (b) the initial elastic deformation, (c) the phase separation between a rubber particle and the homopolymer matrix, and (d) the yielding point.
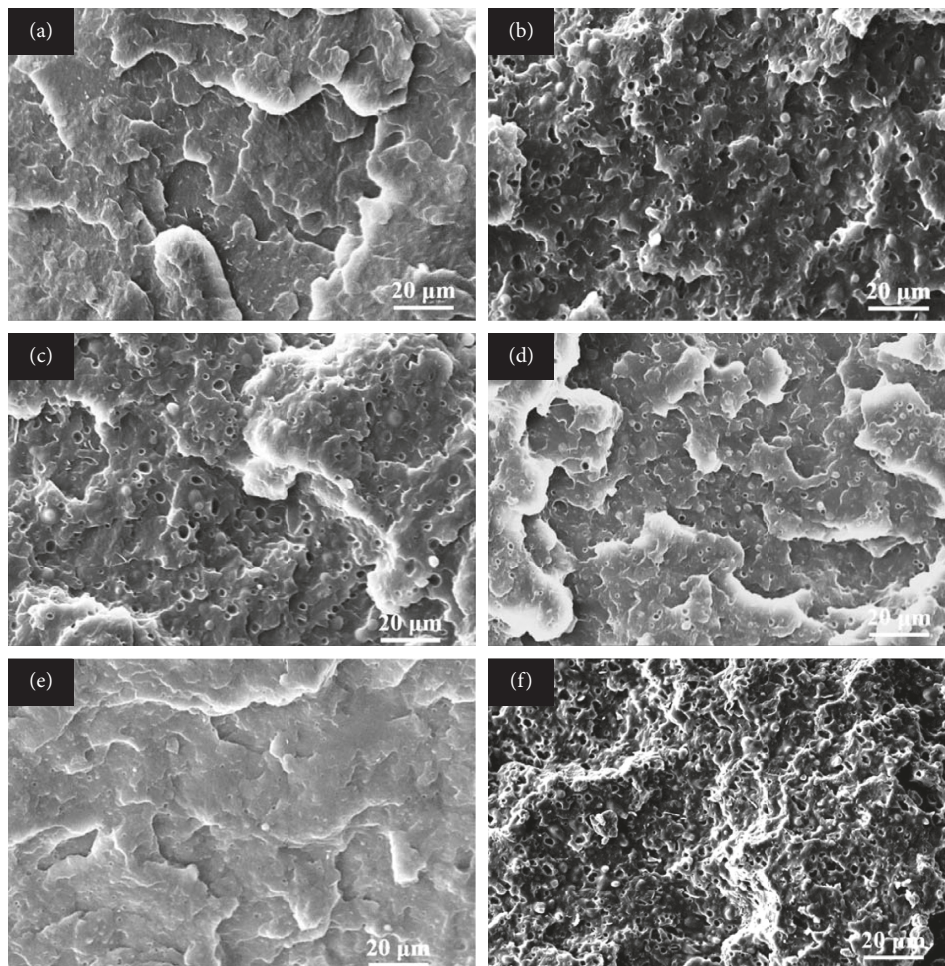
FIGURE 3: The SEM micrographs of the fracture surfaces of ICPP and HPP mixtures: (a) HPP, (b) 20 wt.% ICPP, (c) 40 wt.% ICPP, (d) 60 wt.% ICPP, (e) 80 wt.% ICPP, and (f) 100 wt.% ICPP.
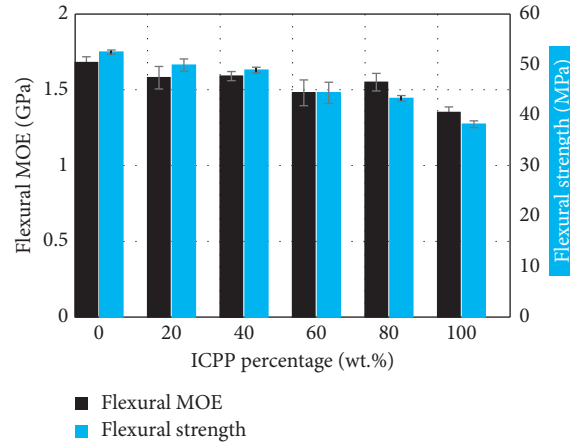
FIGURE 4: The flexural properties of the mixtures of HPP and ICPP.
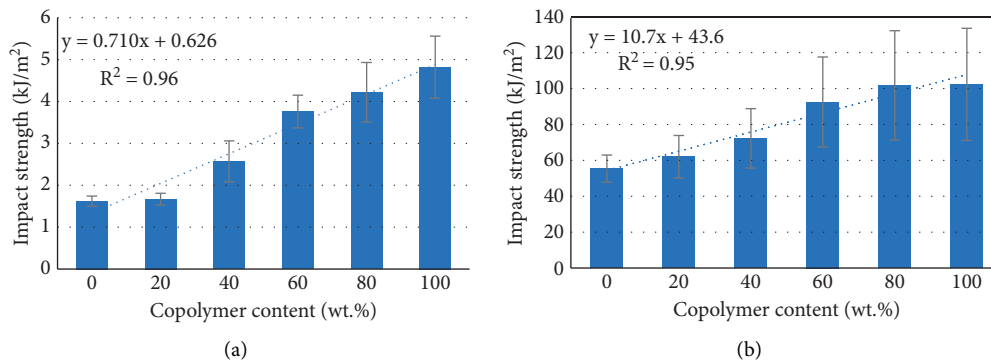
FIGURE 5: The impact properties of the mixture of HPP and ICPP: (a) notched and (b) unnotched.

mixtures have notched impact strengths of 2.57, 3.76, and 4.22 kJ/m^2, which are all significantly greater than those of pure HPP. The fracture surface after the impact test is shown in Figure 3. With rubber particles embedded in the mixtures, the fracture path during the test changed when compared with HPP. The interfacial separation between rubber particles and the homopolymer phase PP occurred and fracture surfaces with exposed rubber particles were observed. Under this circumstance, a greater surface area was created, potentially demanding higher energy in this process. A higher content of rubber particles needs greater energy. Therefore, the impact strengths were observed to increase with increasing rubber particle contents. Another factor that needs to be considered in this process is associated with the interfacial surface energy between rubber particles and homopolymer phase PP. The overall energy used to create the mixture fracture surface, including the energy used to separate rubber particles from homopolymer phase PP, should be greater than that used for creating a pure homopolymer fracture surface to increase the tested impact strength.

That is true for the mixtures with ICPP contents of 40, 60, and 80 wt.%. At the ICPP content of 20 wt.%, the overall energy consumed to create the fracture surface area of the mixture specimens is comparable with that used to create the fracture surface area of HPP specimens.

The unnotched impact strength is much higher than that of the notched impact strength for the same sample. The energy used to initiate the fracture of the specimens is included in the unnotched impact test. With the addition of the ICPP in HPP, the unnotched impact strength of the mixture increased significantly when the ICPP contents in the mixture are at 60 and 80 wt.% (Table 1). At the same time, the unnotched impact strengths at ICPP contents of 60 and 80 wt.% are not significantly different than those of ICPP. When the ICPP contents in the mixture are at 20 and 40 wt.%, the unnotched impact strengths are not significantly greater than those of HPP (Table 1).

A regression analysis of the notched and unnotched impact strengths was conducted and the equations representing the relationships are shown in Figure 5. A good linear relationship with a relatively high coefficient of determination (R^2) was obtained for both notched and unnotched impact strengths as the ICPP contents in the mixtures increased from 0 to 100 wt.%. After mixing HPP and ICPP, the mixture impact strength can be predicted using a linear model based on the initial material properties of the individual components. The melt flow indices of all the mixtures are shown in Table 1. ICPP has a relatively higher melt flow index than that of HPP. Adding ICPP into HPP increased the melt flow index with increasing ICPP contents.
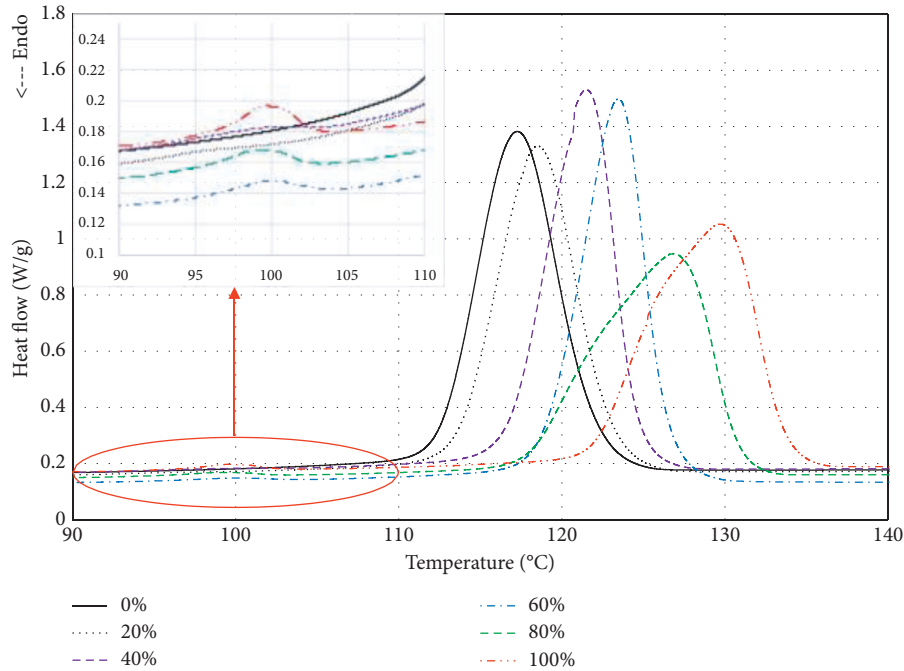
FIGURE 6: DSC cooling scanning curves of the mixtures with ICPP contents of 0, 20, 40, 60, 80, and 100 wt.%.
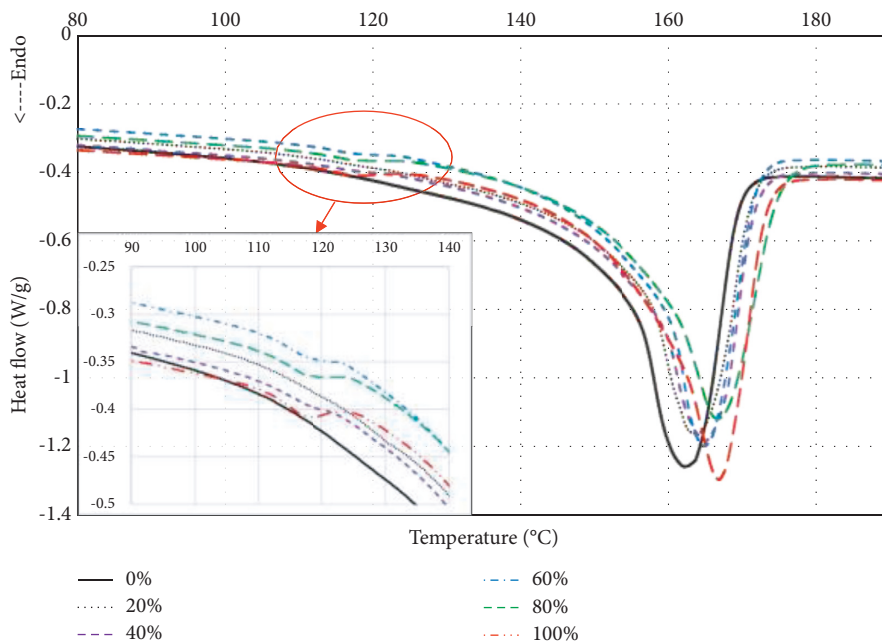
FIGURE 7: DSC second heating scanning curves of mixtures with ICPP contents of 0, 20, 40, 60, 80, and 100 wt.%.

3.3. Thermal Properties. The thermal properties of ICPP, HPP, and the mixtures of the two were characterized using DSC and TGA. The DSC curves of cooling and second heating are shown in Figures 6 and 7, respectively. Cooling of all the specimens in DSC tests was performed at 5°C/min and heating was conducted at 10°C/min. During the cooling process, one peak was observed for the HPP with the onset crystallization temperature of 115°C and the peak crystallization temperature of 117°C (Figure 6 and Table 2). For ICPP, two crystallization peaks were observed (Figure 6).

The first peak occurs at around 100°C and the second peak at around 132°C. The first peak is associated with the crystallization process of the rubber particles in ICPP and the second peak is related to the crystallization process of the homopolymer phase of PP in ICPP. Adding ICPP into HPP did not change the first crystallization peak temperature in the mixtures (Figure 6). At 20 wt.% ICPP, the crystallization peak for the rubber particles is hard to be discerned in the DSC measurement (Figure 6). The crystallization peaks linked to the rubber particles in the mixtures with the ICPP

TABLE 2: The thermal properties of HPP, ICPP, and the ICPP and HPP mixtures.

Sample (%)	DSC									TGA
	1st cooling				2nd heating					
	1st peak	2nd peak			1st peak	2nd peak				
	Enthalpy (J/g)	Onset T (°C)	Peak T (°C)	Enthalpy (J/g)	Enthalpy (J/g)	Onset T (°C)	Peak T (°C)	Enthalpy (J/g)	Crystallinity (%)	Temperature at 5% mass loss (°C)
0	0	115 ± 0.2	117 ± 0.2	94 ± 1	0	152 ± 1	163 ± 2	91 ± 1	44	365 ± 2
20	0	116 ± 0.3	118 ± 0.3	88 ± 1	0	153 ± 1	164 ± 1	87 ± 1	42	378 ± 1
40	0.29 ± 0.03	119 ± 0.5	121 ± 0.7	83 ± 2	0.09 ± 0.02	156 ± 1	164 ± 1	85 ± 1	41	382 ± 4
60	0.53 ± 0.03	121 ± 0.5	123 ± 0.5	80 ± 1	0.17 ± 0.03	157 ± 1	164 ± 1	81 ± 1	39	380 ± 1
80	0.78 ± 0.05	122 ± 1.0	126 ± 0.5	80 ± 3	0.46 ± 0.03	156 ± 1	166 ± 1	79 ± 1	38	387 ± 1
100	0.92 ± 0.02	130 ± 0.7	132 ± 0.9	78 ± 1	0.60 ± 0.13	154 ± 2	167 ± 1	71 ± 1	35	384 ± 3
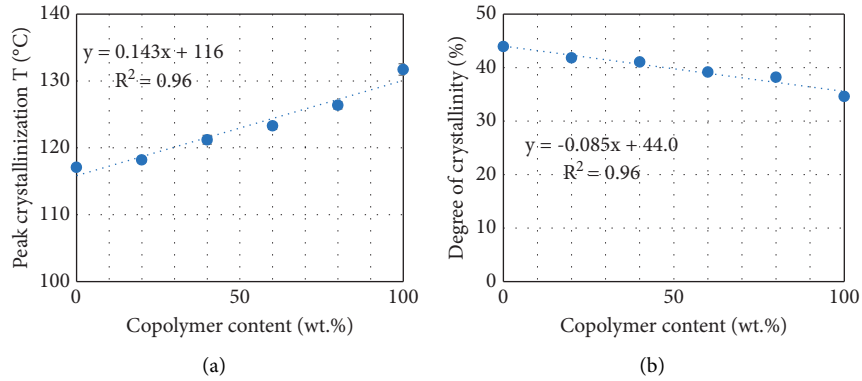
FIGURE 8: Thermal properties of the mixtures of ICPP and HPP showing the relationships of (a) peak crystallization temperatures against ICPP contents and (b) degrees of crystallinity versus ICPP contents.
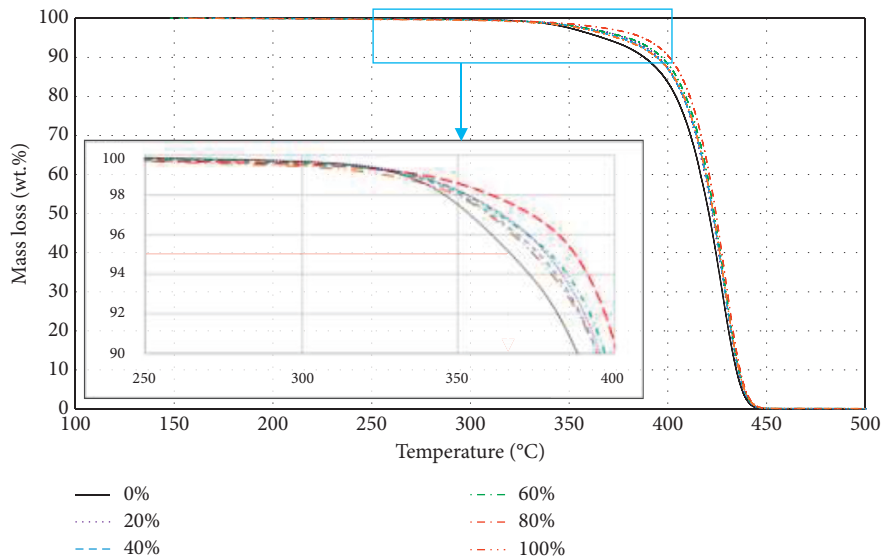
FIGURE 9: The TGA curves of the mixtures with ICPP contents of 0, 20, 40, 60, 80, and 100 wt.%.

contents of 40, 60, and 80 wt.% can be easily identified in Figure 6, and the values of the crystallization enthalpy for these rubber particles in the mixtures changed linearly with the ICPP contents as shown in Table 2.

The second crystallization peak in the cooling process of the DSC measurement is a characteristic of the homopolymer phase PP in ICPP, and the onset and peak crystallization temperatures for the homopolymer phase of PP are 130 and 132°C (Table 2). Adding ICPP into HPP changed its onset and peak crystallization temperatures (Table 2). The possible explanation is that the PP homopolymer molecular structure in ICPP differs from that in the homopolymer phase PP in HPP. The other possibility is that the rubber particles in ICPP might act as heterogeneous nucleating agents and promote nucleation activity. Different nucleation behavior may result from the different sizes of rubber particles in the final mixture, changing the crystallization behaviors of homopolymer phase PP in HPP, including the crystallization rates and crystallite size. A similar particle nucleation effect has been observed in polypropylene

systems [28–30]. More particularly, the peak crystallization temperatures of the mixtures of HPP and ICPP changed linearly with the ICPP contents, and the linear relationship is shown in Table 2 and Figure 8(a). The crystallization enthalpy for the homopolymer phase in the mixture is also shown in Table 2 and the crystallization enthalpy of HPP is 94 J/g while it is 78 J/g for ICPP. The addition of ICPP into HPP decreased the crystallization enthalpy of the homopolymer phase of PP in HPP (Table 2), and the effect is also impacted by the content of ICPP.

The second heating process in the DSC measurement mainly characterizes the melting behaviors of the polymers (Figure 7). HPP showed one melting peak with an onset temperature of 152°C and a peak melting temperature of 163°C. Two melting peaks were observed for ICPP. The lower melting peak is at 117°C and is the melting temperature of the rubber particles in ICPP. This melting peak was observed in the mixtures with ICPP contents of 40, 60, and 80 wt.%. At 20 wt.% of ICPP in the mixture, the melting peak for the rubber particles cannot be identified.

The second melting peak shows the melting point of the homopolymer phase PP in the mixtures, and the melting temperature of the homopolymer phase in ICPP (167°C) is slightly higher than that in HPP (163°C). When different contents of ICPP were embedded in the mixtures, different melting points of the homopolymer phase PP were observed (Table 2). The values of the melting enthalpy for all the samples were collected, and the data are shown in Table 2. The degrees of crystallinity of the mixtures were also calculated based on the melting enthalpy, and the values are shown in Table 2. The degrees of crystallinity of HPP and ICPP are 44 and 35%, respectively. When adding ICPP into HPP with the weight percentages of 20, 40, 60, and 80%, the degrees of crystallinity of the mixtures decreased from 44% for HPP to 42, 41, 39, and 38%, respectively. A linear relationship was also observed between the degree of crystallinity of the mixtures and the ICPP contents in the mixtures as shown in Figure 8(b). The molecular structures of the homopolymer phase PP in ICPP and HPP are different and behaved differently after mixing ICPP and HPP, changing the crystalline structures with different degrees of crystallinity. A lower degree of crystallinity of the homopolymer phase of PP in ICPP decreased the total degrees of crystallinity in the mixtures, changing linearly with increasing contents of ICPP in the mixture according to the rule of mixture. Additionally, the mass percentage of rubber particles increased linearly with the ICPP contents in the mixture, possibly leading to lower degrees of crystallinity.

The thermostability of HPP, ICPP, and their mixtures was investigated using TGA, and the ICPP and the mixtures showed slightly higher thermostability than that of HPP (Figure 9). The temperatures of 5 wt.% mass loss for all the samples are shown in Table 2. The temperature at 5 wt.% mass loss occurred at 365°C for HPP and 384°C for ICPP. Mixing ICPP and HPP changed the temperatures for the mass loss of 5 wt.% for all the mixtures (Table 2), and adding ICPP into HPP increased the temperatures at 5 wt.% mass loss for all the mixtures.

4. Conclusions

Thermal compounding of a commercial grade of HPP with a much higher impact strength of ICPP was conducted using an internal mixer. After thermal compounding, the morphologies of the rubber particles in the mixtures changed, and the final mixture's mechanical behaviors and thermal properties varied with the contents of ICPP in the mixtures. The morphology change of the rubber particle also depends on the loading levels of the rubber particles in the mixtures; i.e., different rubber particle morphologies were obtained with different contents of ICPP in the mixtures.

Adding ICPP into HPP decreased the tensile MOE and the dispersion and distribution of the rubber phase in the mixtures significantly impacted the tensile MOE behaviors. The tensile strength and strain were mainly determined by the weight percentages of the rubber phase and decreased linearly with increasing ICPP contents in this case. Adding ICPP into the HPP increased the notched and unnotched impact strengths, and linear relationships were observed between the notched and unnotched impact strengths and the ICPP contents in the mixtures. The thermal behavior of the mixtures differed with increasing ICPP contents. The peak crystallization temperatures increased linearly with the increasing ICPP contents, and the degrees of crystallinity decreased linearly with the increasing ICPP contents. The thermal behaviors of the rubber phase materials did not change significantly from observations of the DSC and TGA measurements. The homopolymer phase PP in the HPP and ICPP significantly affected the thermal properties of the mixtures due to their differences in molecular structures. With the known properties of HPP and ICPP, the properties of the mixtures of the two can be modeled with the mixing ratios. The selection of HPP and ICPP can be optimized to formulate a specific grade of PP with targeted properties. The mixing process also played a role in determining the final product properties.

Data Availability

No data were used to support this study.

Conflicts of Interest

The authors declare no conflicts of interest.

Acknowledgments

References

[1] A. Dasari, Q. X. Zhang, Z. Z. Yu, and Y. W. Mai, "Toughening polypropylene and its nanocomposites with submicrometer voids," *Macromolecules*, vol. 43, no. 13, pp. 5734–5739, 2010.

[2] B. Z. Jang, D. R. Uhlmann, and J. B. V. Sande, "Rubber-toughening in polypropylene," *Journal of Applied Polymer Science*, vol. 30, no. 6, pp. 2485–2504, 1985.

[3] E. W. Jia, S. J. Zhao, Y. G. Shangguan, and Q. Zheng, "Toughening mechanism of polypropylene bends with polymer particles in core-shell structure: equivalent rubber content effect related to core-shell interfacial strength," *Polymer*, vol. 178, 2019.

[4] J. Z. Liang and R. K. Y. Li, "Rubber toughening in polypropylene: a review," *Journal of Applied Polymer Science*, vol. 77, no. 2, pp. 409–417, 2000.

[5] F. M. Mirabella, "Impact polypropylene copolymers: fractionation and structural characterization," *Polymer*, vol. 34, no. 8, pp. 1729–1735, 1993.

[6] B. P. Panda, S. Mohanty, and S. K. Nayak, "Mechanism of toughening in rubber toughened polyolefin—a review," *Polymer-Plastics Technology and Engineering*, vol. 54, no. 5, pp. 462–473, 2015.

[7] X. D. Wang, H. Q. Li, and R. G. Jin, "Synchronous toughening and reinforcing of polypropylene with ultrahigh-molecular-

weight polyethylene via melt blending: mechanical properties, morphology, and rheology," *Journal of Applied Polymer Science*, vol. 100, no. 5, pp. 3498–3509, 2006.

[8] W. C. J. Zuiderduin, C. Westzaan, J. Huetink, and R. J. Gaymans, "Toughening of polypropylene with calcium carbonate particles," *Polymer*, vol. 44, no. 1, pp. 261–275, 2003.

[9] L. Dorazio, C. Mancarella, E. Martuscelli, G. Sticotti, and P. Massari, "Melt rheology, phase structure and impact properties of injection-moulded samples of isotactic polypropylene/ethylene-propylene copolymer (iPP/EPR) blends: influence of molecular structure of EPR copolymers," *Polymer*, vol. 34, no. 17, pp. 3671–3681, 1993.

[10] F. S. Liao, A. C. Su, and T. C. J. Hsu, "Damping behaviour of dynamically cured butyl rubber/polypropylene blends," *Polymer*, vol. 35, no. 12, pp. 2579–2586, 1994.

[11] P. Wang, Y. L. Qi, and J. Zhang, "Sandwich-structure styrene-butadiene-styrene block copolymer (SBS)/polypropylene (PP) blends: the role of PP molecular weight," *Journal of Materials Research*, vol. 34, no. 6, pp. 982–990, 2019.

[12] M. Yimit, L. Ni, Y. Du, and R. Bkan, "Mechanical and aging properties of polypropylene and styrene-butadiene-styrene composites under outdoor and indoor conditions," *Strength of Materials*, vol. 50, no. 5, pp. 788–799, 2018.

[13] J. G. M. Vangisbergen, H. E. H. Meijer, and P. J. Lemstra, "Structured polymer blends: 2. Processing of polypropylene/EDPM blends: controlled rheology and morphology fixation via electron beam irradiation," *Polymer*, vol. 30, no. 12, pp. 2153–2157, 1989.

[14] L. Dorazio, R. Greco, C. Mancarella, E. Martuscelli, G. Ragosta, and C. Silvesrte, "Effect of the addition of ethylene-propylene random copolymers on the properties of high-density polyethylene/isotactic polypropylene blends: Part 1—morphology and impact behavior of molded samples," *Polymer Engineering & Science*, vol. 22, no. 9, pp. 536–544, 1982.

[15] E. Martuscelli, C. Silvestre, and G. Abate, "Morphology, crystallization and melting behaviour of films of isotactic polypropylene blended with ethylene-propylene copolymers and polyisobutylene," *Polymer*, vol. 23, no. 2, pp. 229–237, 1982.

[16] G. Radonjic, V. Musil, and I. Smit, "Compatibilization of polypropylene/polystyrene blends with poly(styrene-b-butadiene-b-styrene) block copolymer," *Journal of Applied Polymer Science*, vol. 69, p. 2625, 1998.

[17] S. Y. Fu, X. Q. Feng, B. Lauke, and Y. W. Mai, "Effects of particle size, particle/matrix interface adhesion and particle loading on mechanical properties of particulate–polymer composites," *Composites Part B: Engineering*, vol. 39, no. 6, pp. 933–961, 2008.

[18] B. Z. Jang, D. R. Uhlmann, and J. B. V. Sande, "The rubber particle size dependence of crazing in polypropylene," *Polymer Engineering & Science*, vol. 25, no. 10, pp. 643–651, 1985.

[19] M. Ishikawa, "Stability of plastic deformation and toughness of polycarbonate blended with poly(acrylonitrile-butadiene-styrene) copolymer," *Polymer*, vol. 36, no. 11, pp. 2203–2210, 1995.

[20] H. J. Cai, X. L. Luo, X. X. Chen, D. Z. Ma, J. M. Wang, and H. S. Tan, "Structure and properties of impact copolymer polypropylene. II. phase structure and crystalline morphology," *Journal of Applied Polymer Science*, vol. 71, p. 103, 1999.

[21] H. J. Cai, X. L. Luo, D. Z. Ma, J. M. Wang, and H. S. Tan, "Structure and properties of impact copolymer polypropylene. I. chain structure," *Journal of Applied Polymer Science*, vol. 71, p. 93, 1999.

[22] Y. D. Fan, C. Y. Zhang, Y. H. Xue et al., "Effect of copolymerization time on the microstructure and properties of polypropylene/poly(ethylene-co-propylene) in-reactor alloys," *Polymer Journal*, vol. 41, no. 12, pp. 1098–1104, 2009.

[23] Y. C. Peng, M. Musah, B. Via, and X. Q. Wang, "Calcium carbonate particles filled homopolymer polypropylene at different loading levels: mechanical properties characterization and materials failure analysis," *Journal of Composites Science*, vol. 5, 2021.

[24] C. H. Zhang, Y. G. Shangguan, R. F. Chen et al., "Morphology, microstructure and compatibility of impact polypropylene copolymer," *Polymer*, vol. 51, no. 21, pp. 4969–4977, 2010.

[25] Y. Li, J. T. Xu, Q. Dong, Z. S. Fu, and Z. Q. Fan, "Morphology of polypropylene/poly(ethylene-co-propylene) in-reactor alloys prepared by multi-stage sequential polymerization and two-stage polymerization," *Polymer*, vol. 50, no. 21, pp. 5134–5141, 2009.

[26] Z. Q. Fan, Y. Q. Zhang, J. T. Xu, H. T. Wang, and L. X. Feng, "Structure and properties of polypropylene/poly(ethylene-co-propylene) in-situ blends synthesized by spherical Ziegler–Natta catalyst," *Polymer*, vol. 42, no. 13, pp. 5559–5566, 2001.

[27] T. T. Wang and T. K. Kwei, "Effect of induced thermal stresses on the coefficients of thermal expansion and densities of filled polymers," *Journal of Polymer Science Part A-2: Polymer Physics*, vol. 7, no. 5, pp. 889–896, 1969.

[28] J. Kotek, J. Scudla, M. Slouf, and M. Raab, "Combined effect of specific nucleation and rubber dispersion on morphology and mechanical behavior of isotactic polypropylene," *Journal of Applied Polymer Science*, vol. 103, no. 6, pp. 3539–3546, 2007.

[29] M. N. Al-Otaibi, A. Kioul, and S. Al-Zahrani, "Effect of nucleating agent incorporation on mechanical, morphological, and rheological properties of in-situ sopolymer polypropylene and PPH/POE blends," in *Proceedings of the Pps-34: The 34th International Conference of the Polymer Processing Society-Conference Papers*, vol. 2065, Taipei, Taiwan, 2019.

[30] B. Su, Y. G. Zhou, and H. H. Wu, "Influence of mechanical properties of polypropylene/low-density polyethylene nanocomposites: Compatibility and crystallization," *Nanomaterial and Nanotechnology*, vol. 7, 2017.